Available online at www.sciencedirect.com
ScienceDirect
Tectonophysics 466 (2009) 213–228
TECTONOPHYSICS
www.elsevier.com/locate/tecto

Tectonics of the southern tip of the Parece Vela Basin, Philippine Sea Plate

Kyoko Okino [a,*], Yasuhiko Ohara [b], Toshiya Fujiwara [c], Sang-Mook Lee [d], Kin'ichiro Koizumi [a], Yasuyuki Nakamura [a], Shiguo Wu [e]

[a] Ocean Research Institute, University of Tokyo, 1-15-1 Minamidai, Nakano, Tokyo 164-8639, Japan
[b] Hydrographic and Oceanographic Department of Japan, 5-3-1 Tsukiji, Chuo, Tokyo 104-0045, Japan
[c] Japan Agency for Marine-Earth Science and Technology, 2-15 Natsushima, Yokosuka, Kanagawa 237-0061, Japan
[d] School of Earth and Environmental Sciences, Seoul National University, Sillim-dong, Gwanak-gu, Seoul 151-747, South Korea
[e] Institute of Oceanology, Chinese Academy of Science, 7 Nanhai Road, Qingdao 266071, PR China

Received 6 April 2006; received in revised form 22 June 2006
Available online 22 November 2007

Abstract

We report new geophysical and petrological data collected at the southern tip of the Parece Vela Basin in the Philippine Sea. The Parece Vela Basin, which was formed as a backarc basin behind proto Mariana arc–trench system from late Oligocene to middle Miocene, provides us a good opportunity to study the nature of successive backarc basin formations in the Philippine Sea and the relationship between arc and backarc magmatisms. Regional bathymetric map derived from satellite altimetry shows that the southern tip of the basin, now located just west of the Yap arc–trench system, has unique morphological and tectonic features which include: 1) the absence of spreading center or its trace, 2) shallow average depth, and 3) enigmatic curved structures. Our newly collected high-resolution bathymetric data reveal that the spreading fabric similar to the central Parece Vela Basin exists to the north of 9°20′N. Thus it appears that the present-day Yap arc and backarc region represent the western half of the seafloor that was produced by the early E–W and the following NE–SW spreading in the northern and central Parece Vela Basin, and that the eastern counterpart now lies west of the West Mariana Ridge. Unlike the northern Parece Vela Basin, there appears to be no evidence for a systematic propagation of spreading center in the southern part. Instead two rift segments, one which extends from the central Parece Vela Basin and the other which lies within the western remnant arc (Kyushu–Palau Ridge), overlap at the southern tip of the basin, producing a complex seafloor that includes curvilinear deeps and deformed topographic highs.

Keywords: Backarc spreading; Geophysical mapping; Rock geochemistry; Philippine Sea

1. Introduction

The Philippine Sea Plate consists of active and inactive island arcs and backarc basins. Though the origin of the West Philippine Basin is still being debated ("entrapped piece of a large oceanic plate": Hilde and Lee, 1984; or "backarc basin": Hall et al., 1995; Deschamps and Lallemand, 2002), the eastern half of the Philippine Sea Plate was formed by successive events of arc volcanism and backarc magmatism (e.g., Karig, 1971; Okino et al., 1999). According to the present-day configuration, regions of active backarc extension, including the Izu–Bonin incipient rift zones (Taylor et al., 1991) and the Mariana Trough (Martinez et al., 1995, 2000; Yamazaki et al., 2003), are located just west of the arc volcanic front. Recent studies have shown that the Shikoku Basin (SB) and Parece Vela Basin (PVB) are extinct backarc basins formed during late Oligocene to middle Miocene in Izu–Bonin–Mariana (IBM) arc system (Okino et al., 1994, 1998, 1999; Sdrolias et al., 2004). Geologic clues for early development of backarc basin are usually found along the edges of backarc basins. Some of the common features there include remnant arcs and seafloor manifestations of early rifting and spreading. Many features display variable influence of arc volcanism and magmatism. The eastern Philippine Sea offers a

* Corresponding author. Ocean Research Institute, University of Tokyo, 1-15-1 Minamidai, Nakano, Tokyo 164-8639, Japan. Tel.: +81 3 5351 6446; fax: +81 3 5351 6438.
E-mail address: okino@ori.u-tokyo.ac.jp (K. Okino).

0040-1951/$ - see front matter © 2007 Elsevier B.V. All rights reserved.
doi:10.1016/j.tecto.2007.11.017

great opportunity to investigate the evolutionary cycle of the arc system and the mechanism of backarc basin formation in detail, especially those processes related with the initiation and cessation of backarc spreading.

Compared with the well-studied active IBM arc and the SB, few surveys have been carried out systematically in the southern PVB. In the SB, the fan shape of the basin and the analysis of magnetic anomalies indicate that the backarc spreading began in the north and propagated southward (Okino et al., 1994). Tamaki (1992) suggested that the northern edge of the SB acted as a transform-fault-type plate boundary during the basin formation and that the divergent motion in the SB was compensated by strike–slip motion along the edge. Furthermore, he argued that backarc spreading generally initiates from a transform fault.

The northern PVB shows evidences for northward spreading propagation (Okino et al., 1998). However, it is unclear if the spreading started at the southern strike–slip boundary and then propagated toward north, or if it started at the central part and then propagated bilaterally. The southern PVB is also unique in its tectonic setting. The central PVB is divided into east and west by a spreading axis, which is presently extinct. This extinct plate boundary continues farther south, but not as a spreading axis but as the Yap Trench (Ohara et al., 2002). The basin west of the Yap Trench shows no trace of fossil rift axis. Unlike PVB to the north, the area was affected by the collision or subduction of the Caroline Ridge from east (McCabe and Uyeda, 1983; Fujiwara et al., 2000; Lee, 2004). However, there are important gaps in our knowledge about the collision event and its influence on the tectonic evolution of the southern PVB. Because the southern PVB represents the youngest part of the PVB, a detailed investigation of this region will provide new understanding of the Philippine Sea development as well as the mechanism of backarc basin initiation.

This paper is based on our recent survey at the southern tip of the PVB. This is the first time that multibeam echosounder has been deployed in this area, although the coverage was not complete. First we describe the morphological features, and the characteristics of gravity and magnetic anomalies. This is followed by an interpretation on different parts of the survey area. Finally, an evolution model of the southern tip of the PVB is provided where we compare the southern Mariana Trough with other modern analogues.

2. Tectonic setting

Fig. 1 shows the tectonic setting around the Philippine Sea and main morphological features. The SB and the PVB formed from late Oligocene to middle Miocene as backarc basins behind the proto IBM arc (Okino et al., 1999). The proto IBM arc crust rifted and split into two parts as the new oceanic crust was produced along the backarc spreading center. The western fragment of the arc later became what we call the Kyushu–Palau Ridge (Karig, 1971; Haraguchi et al., 2003). After the formation of SB and PVB, the next stage of backarc volcanism constructed en-echelon chains of seamounts (the Nishi–Shichito Ridge and the West Mariana Ridge) (Hochstaedter et al., 2000; Ishizuka et al., 2003; Machida and Ishii, 2003), which covered the eastern part of the SB and PVB. Behind the present-day southern IBM arc, the Mariana Trough began to open as a backarc basin at about 6 Ma (Hussong and Uyeda, 1981; Iwamoto et al., 2002). The northern IBM arc is still in the incipient rifting stage (Taylor et al., 1991).

At 24°N, the Kyushu–Palau Ridge (KPR) changes its direction from NNW–SSE to NNE–SSW (Fig. 1). The northern KPR consists of a relatively linear ridge, whereas the southern KPR consists of discrete seamounts on a shallow platform. The eastern flank of the KPR exhibits numerous linear fault escarpments, which are interpreted as rift walls formed at the start of backarc opening. In some places, syn-rift basins are located along the escarpments (Ohara et al., 1997). Sometimes volcanic cones overprint the basin floor. The western flank of the KPR contains en-echelon chains of seamounts similar to the Nishi–Shichito Ridge. The seamount chains extend into an older part of the seafloor in the western Philippine Sea (Tokuyama, 1995). The existence of thin layer of a P-wave velocity of 6 km/s, according to seismic refraction profiles by Shinohara et al. (1999) as well as the presence of tonalitic rocks recovered from the northern KPR (Haraguchi et al., 2003), suggest that the crust has the characteristics of an island arc. The latest volcanism along the KPR is dated as 27–25 Ma (Ishizuka, personal communication), which is consistent with the age of initiation of backarc opening in the Shikoku Basin derived from magnetic anomalies (Okino et al., 1994); the oldest anomaly, chron 7, corresponding to 26 Ma (Cande and Kent, 1995).

The formation of PVB occurred during two different spreading episodes. The western PVB displays N–S trending abyssal hills, those are parallel to the strikes of magnetic anomalies, indicating E–W spreading during the early stage of basin formation. The age of spreading initiation is still uncertain because of the lack of dense magnetic survey in the southern part of the basin. Okino et al. (1998) suggests that the spreading started at 26/27 Ma in the northern PVB, where the width of the basin is narrower than the central PVB. Sdrolias et al. (2004) identifies the oldest magnetic anomaly in the southern PVB as chron 9, corresponding to 28 Ma. The spreading direction then rotated anti-clockwisely at 19/20 Ma (Okino et al., 1998). The central part of the PVB is characterized by a highly segmented rift system (the Parece Vela Rift), which is currently bounded by prominent NNE–SSW fracture zones. This rift consists of N–S aligned rhomboidal depressions along which oceanic core complexes are sometimes present (Ohara et al., 2001, 2003). The exact age of spreading cessation is not certain. However, the recent dating of a rock sample recovered at the Parece Vela Rift (PVR) indicates a possible cessation of the spreading at about 11 Ma. The N–S trending magnetic anomalies in the northwestern PVB abut the KPR rift wall, which may be interpreted as a sign that the rifting and spreading propagated toward the north during the first stage of basin formation. The southern part of the PVB has not been fully mapped yet. Recent surveys have only covered the PVR and the adjacent region, where highly segmented rift system with severe deformation presumably by an oblique extension has been recognized (Ohara et al., 2005).

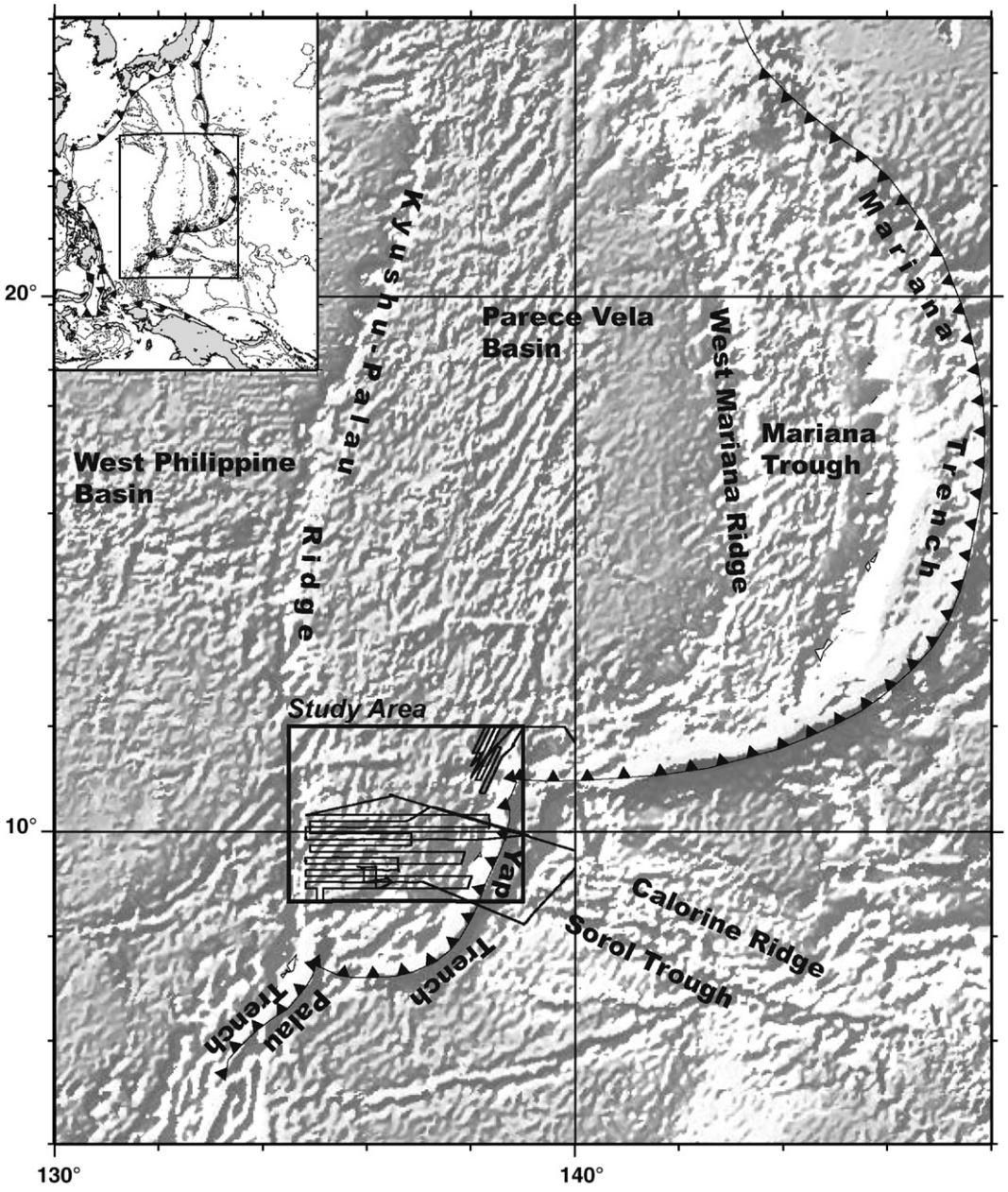

Fig. 1. Regional map showing morphological features of the Parece Vela Basin and the surroundings. ETOPO2 bathymetry data are used. Thin black lines indicate survey lines conducted during KH05-1. Box marks the area shown in Figs. 2, 3 and 4.

To the north of 11°N, past studies suggest that the PVB developed from the division of the proto-Mariana arc (e.g., Mrozowski and Hayes, 1979). This region which currently lies between the KPR and the West Mariana Ridge to the north of 11°N shall be referred to the main PVB in this study. The tectonic setting south of 11°N differs from that of the main PVB. According to regional bathymetric map (Fig. 1), the southernmost PVB lies between the KPR and Yap Trench. It is worth noting that here the rift system of PVR evolves into a subduction zone (Ohara et al., 2002). Along the Yap Trench, the convergence rate varies with respect to the Sorol Trough, since it marks a transtensional boundary between the Pacific and Caroline plates (Lee, 2004). North of the Sorol Trough, GPS measurement reveals a convergence rate of 10 mm/yr (Kotake, 2000), which is less than half the value that predicted by global plate model (Seno et al., 1993). South of the Sorol Trough, the convergence occurs at a slower rate or may have even stopped (Lee, 2004). The seismicity along the Yap Trench is low, and there is no evidence for the presence of a Wadati-Benioff zone extending beyond several tens of kilometers from the seafloor. The bathymetric high that emerges at the Yap Island extends along the landward side of the trench, however, the proximity of the arc to the trench (~50 km), the presence of metamorphic rocks on Yap Island as well as the absence of active arc volcanism do not match with typical arc–trench systems where the bathymetric high often relates to an active island arc. The backarc side of the Yap arc–trench system is even more enigmatic. The area seems to be the southward prolongation of

the main PVB. However, no traces of extinct spreading center can be recognized at least on the regional map derived from satellite altimetry. McCabe and Uyeda (1983) suggest that the Caroline Ridge collided with the Yap Trench in the early Miocene, and that this collision caused the volcanic activity in the Yap Arc to stop. Fujiwara et al. (2000) compiled geophysical data acquired along the Yap Trench and provided a more updated scenario of tectonic evolution. According to their model, the collision of the Caroline Ridge along the Yap Trench caused the cessation of arc volcanism and the tectonic erosion of the Yap forearc. The collision also contributed to present-day configuration where the Yap 'arc' mainly consists of obducted oceanic crust.

Important issues that need to be resolved in this paper are whether the southernmost PVB has similar tectonic features as those to the north, and if not, how different is it from the north and what is the cause of the difference.

3. Data acquisition and processing

We acquired high-resolution multibeam swath bathymetry, marine gravity and magnetic field data over the southern tip of the Parece Vela Basin west of the Yap Trench in 2005 using R/V Hakuho-Maru (KH05-1). A multi-channel seismic profile across the northern Yap Trench was also obtained during the cruise. The track lines were laid out E–W from the KPR to the Yap arc. Track spacing was 14 and 7 nautical miles in the eastern and western parts of the survey, respectively (Fig. 1).

Swath bathymetry data were collected with the Sea Beam 2120 system, which operates at 20 kHz and comprises of 120 beams at the surveyed depths. The horizontal resolution ranges 35–85 m, and the average swath width is approximately 11 km. The sound velocity near the sea surface was corrected using real-time data from the surface water velocity meter, and in depth using Expendable CTD (XCTD) and Expendable Bathythermograph (XBT) that were deployed at several locations during the cruise. The newly acquired data were merged with swath bathymetry acquired in previous cruises (KH92-1, YK93-03, YK95-06 and YK96-12) to produce a gridded map (Figs. 2 and 3). The grid interval is 100 m, and the dataset is masked to approximately the original swath coverage allowing interpolation of small gaps within 1 km. By combining JTOPO1 (digital 1 arc-min bathymetry grid for northwestern Pacific produced by Marin Information Research Center, http://www.mirc.jha.or.jp/en/index.html;), a complete bathymetric grid without gaps but with reasonable spatial resolution was produced in order to investigate the regional tectonic features and to perform subsequent potential field analysis. No adjustment among datasets was necessary during

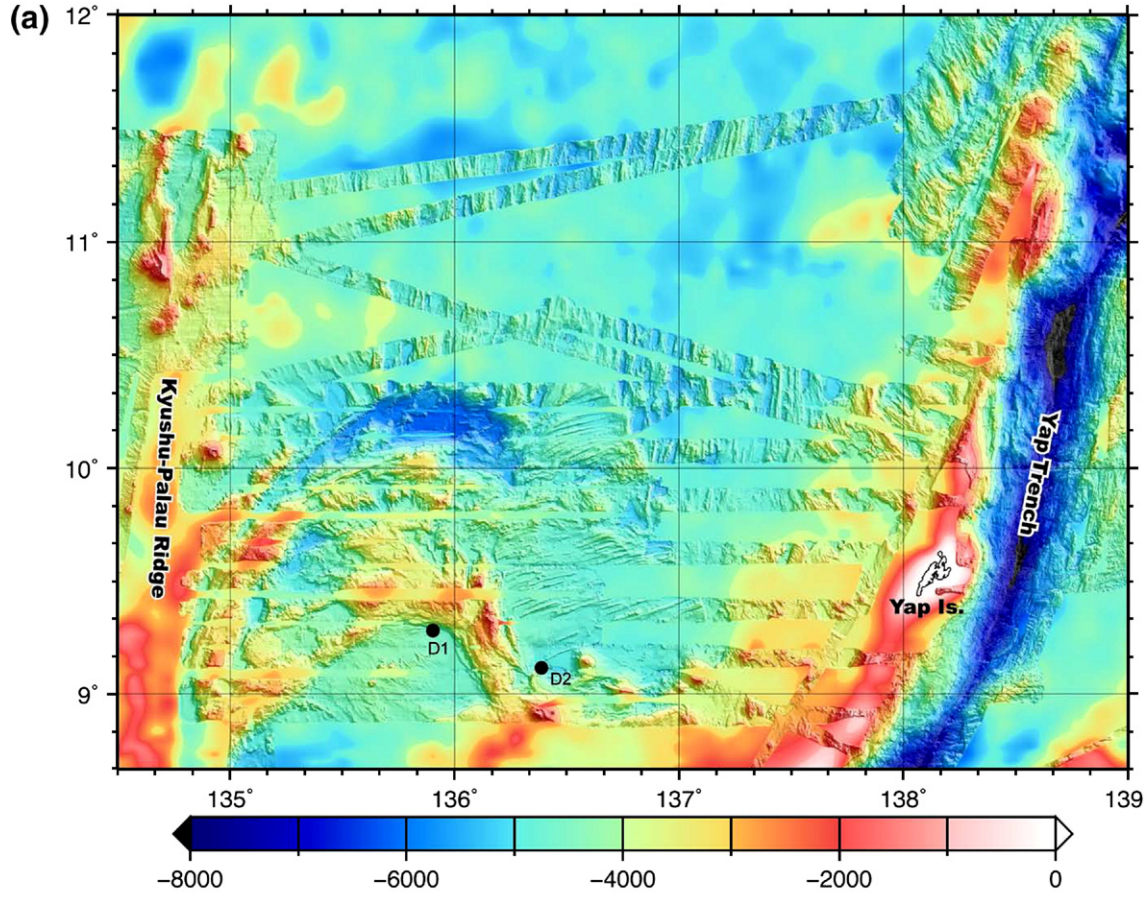

Fig. 2. (a) Shaded relief with bathymetry contours in the southern tip of the Parece Vela Basin, located between the Kyushu–Palau Ridge and the Yap arc–trench system. Swath data collected during previous cruises are combined. Bathymetry is illuminated from directions 0° and 090°. Areas outside swath coverage are colored but without illumination. Solid circles are the loci of dredge hauls. (b) Tectonic features superimposed on shaded bathymetry.

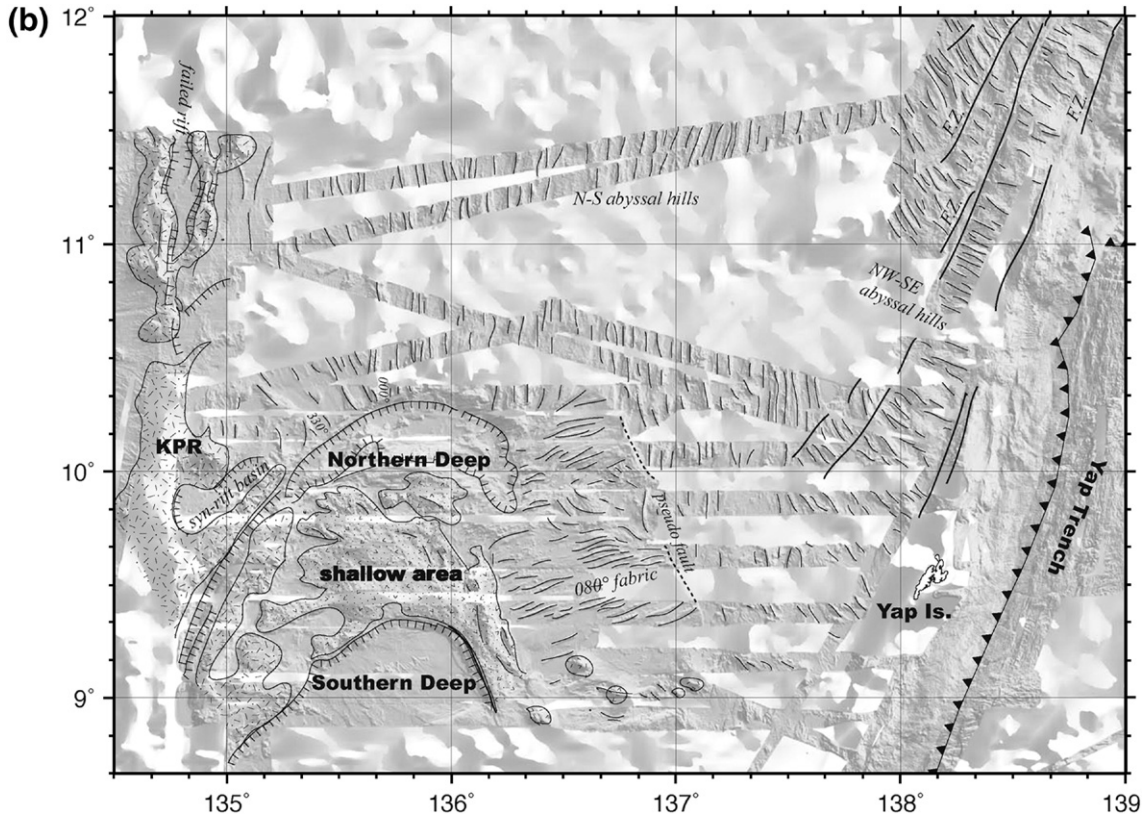

Fig. 2 (*continued*).

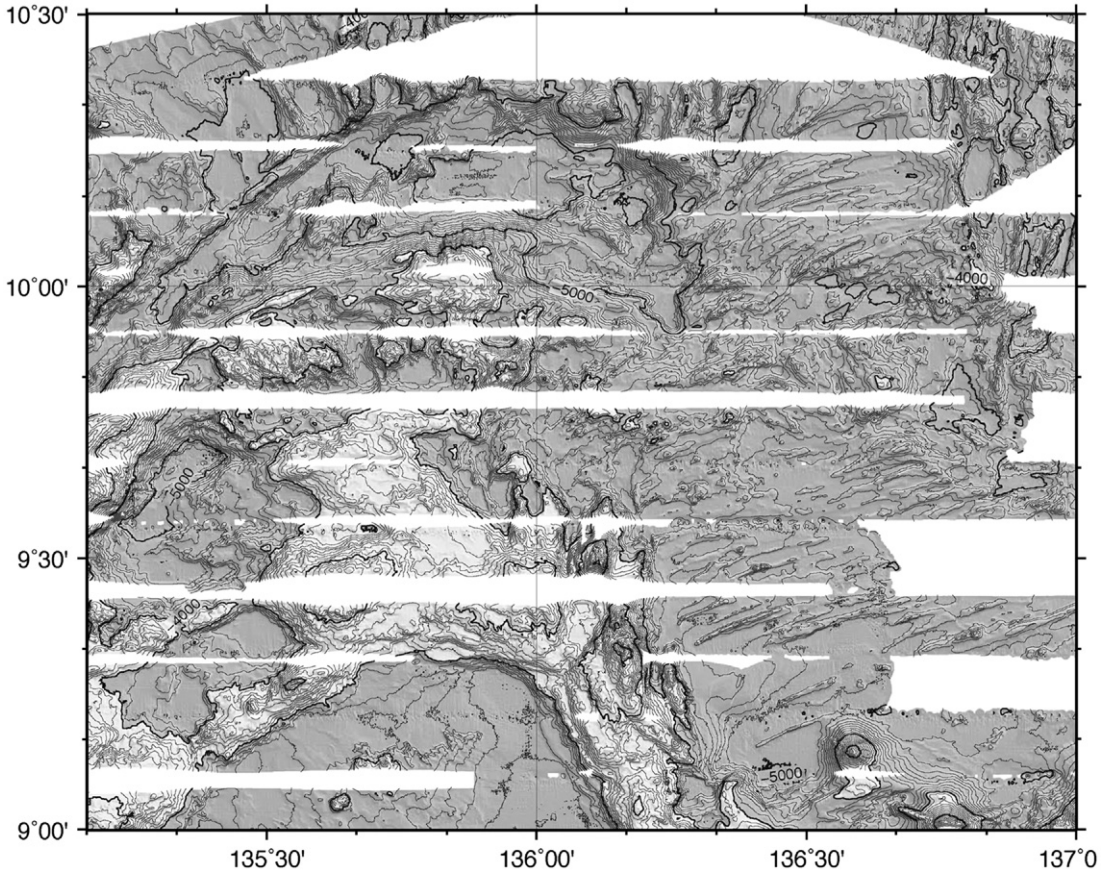

Fig. 3. Close up view of two deeps and a relatively shallow area with multiple topographic highs. Contour interval is 100 m.

compilation as the difference between newly collected data and previous data was negligible.

Gravity data were acquired using a Lacoste–Romberg type shipboard gravity meter (ZLS-D004). Drift and Eötvös corrections were made, and the free-air gravity anomaly was calculated by subtracting the shipboard gravity using Gravity Formula 1980. The root-mean square crossover (rms) errors is 1.2 mGal over 25 points. Satellite gravity data (Sandwell and

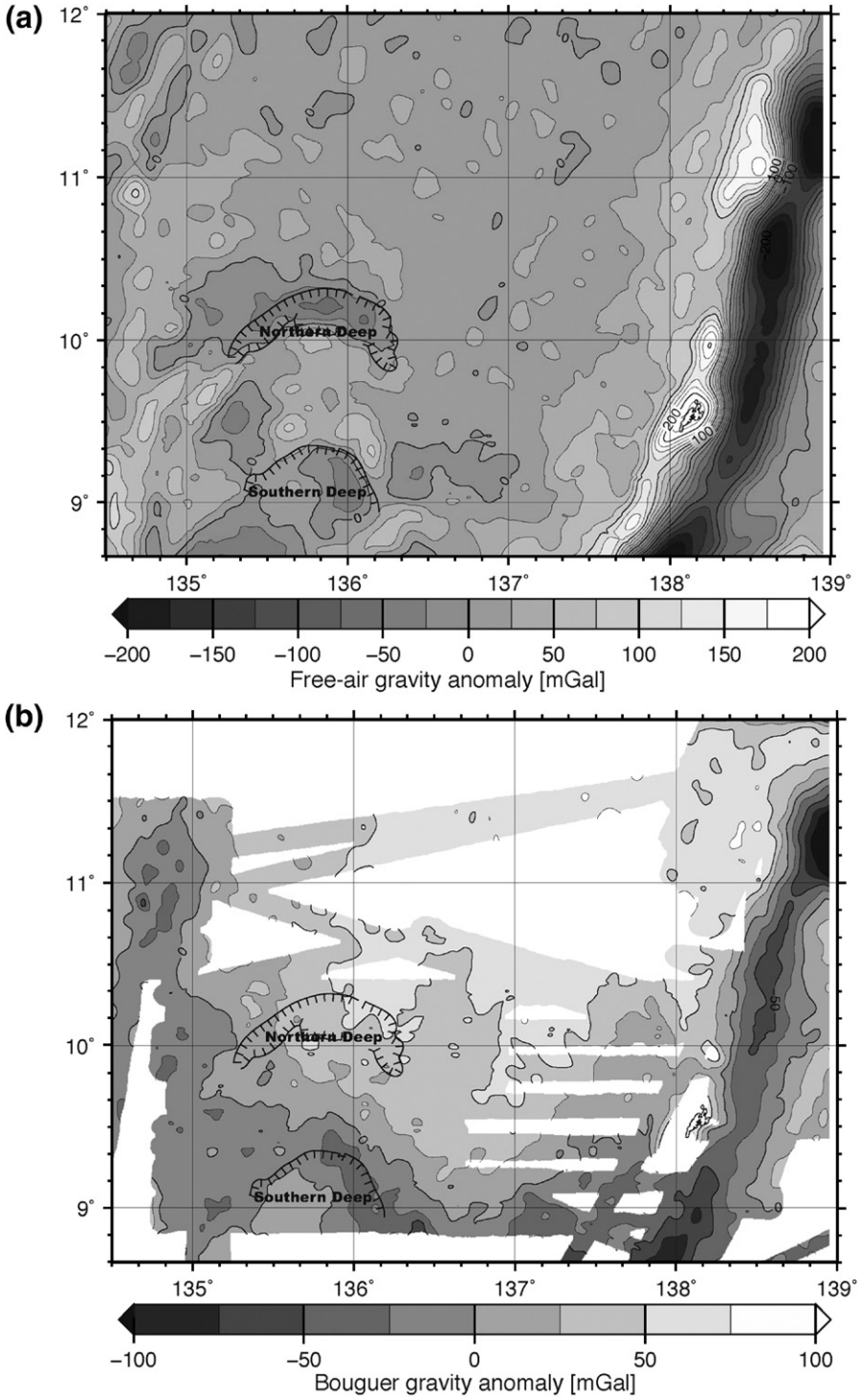

Fig. 4. (a) Free-air gravity anomaly map compiled from shipboard and satellite altimetry derived values. Contour interval is 25 mGal. (b) Bouguer gravity anomaly map calculated using a density contrast of 1720 kg/m^3 for the seafloor variation, which removes most of the short-wavelength anomalies. Contour interval is 25 mGal. (c) Crustal thickness distribution assuming Airy isostacy. Densities of 1030, 2750, 3300 kg/m^3 for water, crust, and mantle are assumed. The calculation also assumes that seafloor at a depth of 5000 m has a crustal thickness of 6 km. Contour interval is 3 km. The areas along the Yap Trench is masked. (d) Isostatic residual anomaly map calculated by subtracting the gravity effect of an Airy Moho interface from the Bouguer anomalies. The contour interval is 25 mGal. The areas along the Yap Trench is masked.

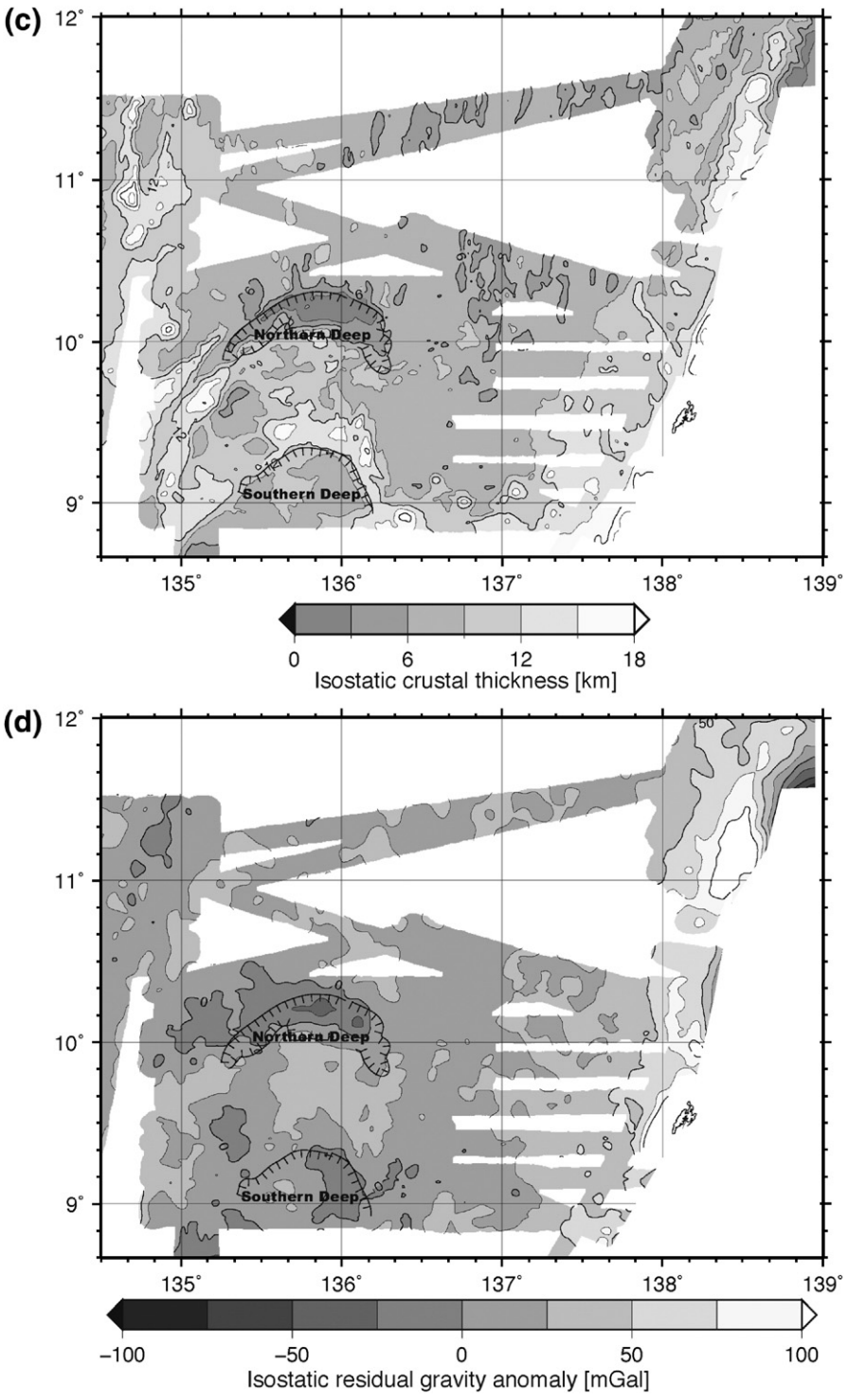

Fig. 4 (*continued*).

Smith, 1997) were merged to fill the data gap, and to eventually produce a 500 m cell size grid map (Fig. 4a).

In order to constrain the subsurface density structure of the area of interest, we calculated the Bouguer anomalies (Fig. 4b) by subtracting the predicted gravity effects of seafloor relief from the observed free-air gravity anomaly. Airy isostatic crustal thicknesses were also calculated from bathymetric map assuming that the seafloor at 5 km depth has a crustal thickness of 6 km (Fig. 4c). We assumed that water/crust and water/mantle density contrasts are 1720 kg/m^3 and 2270 kg/m^3, respectively. The gravitational effect associated with the undulation of Moho was then calculated using the 3-D Fourier method (Parker, 1972), which was then removed from the Bouguer anomaly to produce the isostatic residual anomaly (Fig. 4d). Because the calculations were based on local isostasy, the results include effects arising from non-isostatic structural

variation in the crust and uppermost mantle. The ignorance of non-isostatic effect is the most noticeable where the slab subducts along the Yap Trench.

The magnetic field data were acquired every 30 seconds using a surface-towed proton precession magnetometer (PR-745, Kawasaki Geol. Eng. Co.). The long-wavelength variation was removed from the data using International Geomagnetic Reference Field ver. 9 (Macmillan et al., 2003) to obtain magnetic anomalies. The daily mean values of the geomagnetic field disturbance levels in the two horizontal field components observed at selected stations, expressed as Kp index, were moderate during our survey. However, the crossover errors were large with an rms error of 37 nT. The closest available magnetic observatory is at southern Japan (Kanoya, 31°25′N, 130°52′E) more than 2000 km northwest of the survey area, such that no appropriate diurnal correction could be obtained using the station data. We had to shift the Kanoya station magnetic data, taking into account the time lag at the survey area, and then calculated our geomagnetic variation model using a stochastic inversion to minimize crossover errors. This correction reduced the rms cross over errors to 15 nT. We did not calculate crustal magnetization because data distribution is too sparse to produce magnetic anomaly grid at meaningful grid interval.

We performed two dredge hauls during the cruise (Fig. 2(a), Table 1). Heavily weathered pillow basalts were recovered from dredge site D1, which are described in Section 4.4. However, we failed to obtain rock samples from D2 site.

Seismic reflection profile was also acquired using a total 57-liters air-gun array and 48-channel solid-state streamer. The line crossed the Yap Trench, arc and backarc regions, and total length of the profile was approximately 180 km (Fig. 1). However, the result of seismic survey is beyond the scope of this paper.

4. Results

4.1. Morphological features

Fig. 2(a) shows the bathymetry of the southern tip of the PVB between the Yap Trench and the KPR. Our interpretation of the major morphological and tectonic features is drawn in Fig. 2(b). A close up view of the central part of the study area is shown in Fig. 3. The study area can be divided into four regions based on major topographic features and fine-scale seafloor fabrics.

(1) Along the Yap Trench, an area shallower than 3800 m stretches approximately 90 km to the west of the trench axis. This area is characterized by short segments of NW–SE trending abyssal hills, which are well defined to the north of the Yap Island. The abyssal hills are cross-cut and offset by several NE–SW trending fracture zones. They likely developed during the final stage of PVR formation when spreading was occurring in the NE–SW direction. The NW–SE abyssal hills were then presumably the three or four southernmost spreading segments in the PVB. The average depth in this area becomes shallower southward and eastward.

(2) Another region with unique seafloor fabric lies to the west of NW–SE abyssal hills. This region is characterized by N–S well-organized seafloor fabric, which is likely formed by E–W spreading during the early stage of PVB formation. The water depths range from 3800 to 5200 m. A typical abyssal hill has a relief of less than 1000 m, however the basement relief might be larger taking into account the sediment between the abyssal hills. Unlike the highly segmented NW–SE abyssal hills to the east, no fracture zones is observed, such an absence of fracture zones is typical of the western half of the main PVB. The transition zone between N–S and NW–SE fabric is not marked by any distinct structural unit or by sudden change in seafloor depth. Such an observation suggests that a continuous reorientation of the stress field occurred between the E–W opening and NE–SW opening episodes. West of 135°40′E, the seafloor fabric gradually changes its trend from N–S to NNW–SSE. This fact reflects a variation in the spreading direction during the initial stage of the spreading. Such a variation has not yet reported in the main PVB, therefore it might be due to the complex geometry at the tip of the basin. In our survey area, the KPR becomes less prominent compared to the north, and loses its ridge-like morphology (Fig. 1). And the transition between the remnant arc and backarc basin is characterized by a complex morphologies. An N–S linear depression can be seen along 134°50′E from 11°N to 11°30′N and divides the KPR. We infer that it is a trace of failed rift, which probably formed during the early stage of E–W backarc rifting and spreading.

(3) Another prominent morphological features in the survey area are two sharp, curvilinear deeps east of the KPR (Figs. 2 and 3). The deepest one is located at 10°15′N (Northern Deep in Fig. 2(b)) and the other one at 9°15′N (Southern Deep in Fig. 2(b)). Both are convex towards the north. The Northern Deep reaches a depth of 6100 m and the southern one 4500 m. The northern edge of the deep is marked by steep fault that cuts across the local N–S

Table 1
List of dredge sites during KH05-1-Leg3 cruise

Dredge site	Start			End			Main lithologies recovered
	Latitude	Longitude	Depth (m)	Latitude	Longitude	Depth (m)	
1	9°17.71′N	135°55.85′N	4292	9°18.77′N	135°56.44’N	3634	Heavily weathered pillow lava
2	9°06.88′N	136°23.17′N	4893	9°06.15′N	136°23.15′N	4511	Mud ball

seafloor fabric. The deep extends southwest as a narrow curvilinear rift trending 030°, which merges with the KPR. A series of rifts that is almost parallel to this curvilinear rift is also observed. The area between the Northern Deep and the Southern Deep is characterized by a relatively shallow seafloor, which itself comprises of several topographic highs. The summit of these highs is less than 2000 m deep, which is almost as shallow as that of the KPR. This shallow, complex structure seems to be volcanic origin, but does not display any widespread abyssal hills. The structure has a curvilinear shape and is convex to north or northeast as a whole, but each topographic highs exhibits somewhat different characteristics: some highs are elongated in E–W direction, whereas some peaks in its eastern branch comprise of N–S trending small ridges. Some linear features observed on this shallow area presumably reflect the presence of faults, suggesting the deformation after or concurrently with the volcanism. South of the survey area, a similar set of curvilinear deep and highs is recognized on the predicted bathymetry around at 8°20′N–8°40′N (Fig. 1).

(4) The seafloor east of curvilinear rifts and shallow area between two deeps mainly consists of 080° trending abyssal hills and includes small blocks having fabric of variable orientation (Fig. 2(b) and Fig. 3). The average relief (~300 m) of the abyssal hills is smaller than in other areas, maybe due to a thicker sediment layer filling the troughs in between the abyssal hills. It should be noted that the 080° fabric is roughly perpendicular to the western curvilinear high. The transition between the 080° fabric and N–S fabric is marked by a NNW–SSE trending pseudofault, which runs between 10°N and 10°20′N. This pseudofault turns into an ambiguous discordant zone farther south. The origin of 080° fabric remains unclear at this stage, however we will discuss this issue in a later section.

4.2. Gravity characteristics and isostatic crustal thickness variations

The basin floor with N–S abyssal hills is characterized by small amplitude in free-air gravity anomalies (Fig. 4a), the total variation is generally less than ±25 mGal. At the scale of the survey area, the gravity anomaly values generally decrease westward away from the arc. For instance, the region near the arc with the NW–SE abyssal hills shows higher free-air anomaly values between 20–60 mGal than those to the west. The region that displays 080° abyssal hills has free-air anomaly values around 0 mGal. Also in our study area, the gravity tends to decrease to 20–30 mGal toward south, despite the decrease in water depth. Such decrease in gravity anomaly may be partly due to a thicker sediment and/or to the thickening of crust (Lee, 2004). Contrary to the continuous high anomaly at the Yap arc (50–200 mGal), the KPR has low free-air gravity anomalies (25–100 mGal) (Fig. 4a). The largest variations can be observed near the southwestern part of the study area, where the curvilinear rifts and complex topographic high are developed. The Northern Deep is accompanied by a low free-air anomaly of ~−50 mGal. The Southern Deep and small syn-rift basins located west of the dome are also associated with −40 mGal low free-air anomalies, although they are shallower than the Northern Deep. The presence of a lower gravity anomaly at the loci of Southern Deep and syn-rift basins may indicate that a thinner crust exists beneath these rifts and/or that sediment that fills these rifts is thicker compared to the Northern Deep. The positive anomaly over the topographic high between two deeps reaches 60 mGal.

Bouguer gravity anomalies (Fig. 4b) show an overall decreasing trend southwestward. The reduced anomalies along the KPR and the southern Yap arc south of the Yap Island indicate thicker crust beneath these highs. The northern curvilinear deep does not exhibit significant Bouguer anomaly, which suggests that the observed gravity value can be explained solely by the seafloor relief. On the other hand, the low Bouguer anomaly south of the northern deep does not coincide exactly with the morphological feature. The anomaly pattern may be related to both a thicker than normal crust beneath the topographic high and/or sediment effect. It should be noted that the northern Yap arc with NW–SE spreading fabric has relatively higher anomalies than the south, which seems to indicate a northward decrease in crustal thickness. Such variation is consistent with hypotheses that the northern Yap arc does not have typical arc crust but is in fact the southern extension of the main PVB.

The inferred crustal thickness assuming Airy isostasy and isostatic residual anomaly are shown in Fig. 4c and d, respectively. If the assumption of Airy isostasy produces small residual anomalies, the predicted crustal thickness variations should match with both the observed bathymetry and gravity anomalies. The regions with large negative residuals (<−40 mGal) coincide with the two curvilinear deeps, and those of large positive residuals match with the basin with NW–SE abyssal hills west of the Yap arc. Such large deviation suggests that the observed gravity anomalies cannot be explained by Airy isostasy. Of course, the isostatic model does not take into account of the thermal structure and dynamic effects. Moreover, we have ignored the effect of sediment thickness in our analysis. Still the positive residuals over the basin with NW–SE lineaments, which is considered to be the southern extension of the main PVB, seems to imply that there may be some dynamical effect related to the subduction zone. Also small residual anomaly around KPR can be considered as being isostatically compensated roughly. At this place, the crust may be 6–20 km thicker than that in the basin floor.

4.3. Magnetic characteristics

The magnetic anomalies along the survey lines are shown in Fig. 5. The correlations among lines are not clear. Such a lack of correlation may be due to the low amplitude of anomalies and sparse line interval. The magnetic amplitude in regions of N–S abyssal hills is less than 100 nT. This can be explained by the presence of magnetic lineation with N–S strike due to E–W spreading near the magnetic equator. In areas of curvilinear rifts and topographic highs, the magnetic amplitude is larger than in

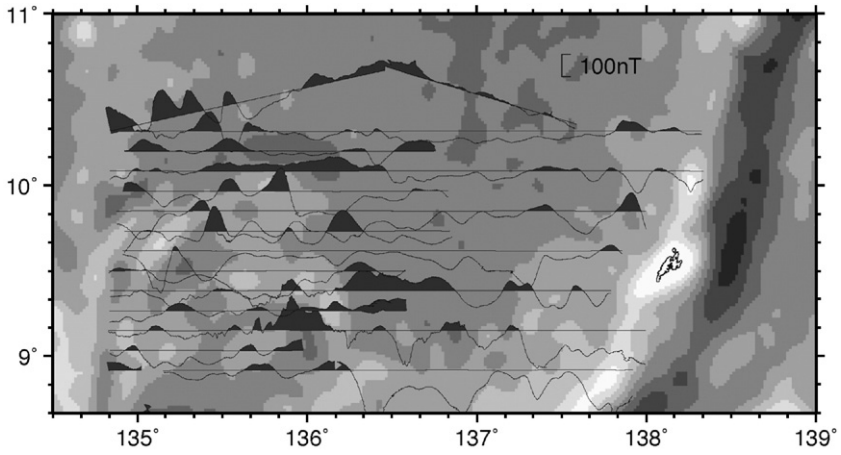

Fig. 5. Magnetic anomaly profiles projected on bathymetry map. Areas greater than −25 nT are shaded black. The inset shows amplitude scale.

northern part of the survey area and shows relatively short-wavelength variation. Though these variations do not correlate well with the observed morphology, we can still recognize some pattern in the anomaly distribution. The shallow area with multiple topographic highs is associated with a large negative value of −250 nT at its northern branch. The positive anomalies, on the other hand, are located both north and south of the negative anomaly. This pattern can be explained by assuming that the magnetization of the shallow area is as same as the present-day ambient geomagnetic field (I=3.6, D=0.9), although we do not know the magnetic field when this shallow area was formed. The high magnetization with respect to the surrounding basin may be due to a thicker source layer. High magnetic anomalies are also observed in the areas of 080° spreading fabric. They may be due to an anomalously thick magnetized layer, but we cannot find significant change of crustal thickness in this area. Another possibility is presence of fractionated melt, which is similar to the model proposed for propagation rift tips (Christie and Sinton, 1981; Sinton et al., 1983; Martinez et al., 1999) , otherwise, the wavelength and amplitude of the anomalies may be due to skew of the magnetic field.

4.4. Petrography and mineralogy of the rock samples

A relatively large amount of heavily weathered pillow lavas was recovered in site D1 in the southern curvilinear deep (Table 1; Fig. 2(a)). Groundmass is so heavily weathered such that no primary microphenocrysts are preserved. However, the relict clinopyroxene phenocrysts are fresh; these are euhedral minerals with less than ~5 mm long. A trace amount of euhedral fresh spinel phenocrysts is also found. The other mineral phases cannot be identified optically.

In order to have a rough idea about the origin of these rocks, we performed microprobe analysis on a selected single thin section. Because of the heavy weathering, it is unlikely that we may obtain meaningful age and isotopic data. Mineral compositions were analyzed with a JEOL JXA8900R electron microprobe at the Ocean Research Institute of the University of Tokyo. The operating conditions were 15-kV accelerating voltage, 12-nA specimen current and 1-μm beam diameter with correction procedure after Bence and Albee (1968). Total Fe is assumed to be equal to Fe^{2+} for clinopyroxene; Fe^{3+} content of spinel was calculated based on stoichiometry. Representative analysis of clinopyroxene and spinel is shown in Table 2.

The clinopyroxene phenocrysts grossly plot in the field of augite (Fig. 6a). No compositional zoning is observed for the analyzed clinopyroxenes. The Mg# (=Mg/(Mg+Fe)) of the clinopyroxene ranges from 0.77 to 0.90 with an average value of 0.84. The spinels have relatively uniform compositions with Cr# (=Cr/(Cr+Al)) 0.78, Mg# 0.64, and TiO2 content 0.24 wt.%.

Kushiro (1960) and Le Bas (1962) showed that Si–Al substitution in clinopyroxene structure is controlled by physicochemical conditions; clinopyroxenes from tholeiitic

Table 2
Representative electron microprobe analysis of clinopyroxene and spinel

	Clinopyroxene	Spinel
(wt.%)		
SiO2	53.07	–
TiO2	0.11	0.24
Al2O3	2.41	9.53
FeO	5.64	12.00
Fe2O3	–	8.23
MnO	0.21	0.25
MgO	17.27	13.61
CaO	20.66	0.01
Na2O	0.18	–
K2O	0.00	–
Cr2O3	0.43	53.66
V2O3	0.00	–
NiO	0.03	0.10
P2O5	0.03	–
Total	100.05	97.63
Mg #	0.845	0.675
Cr #	–	0.791
En	48.9	–
Fs	9.0	–
Wo	42.1	–

En, enstatite content; Fs, ferrosilite content; Wo, wollastonite content.

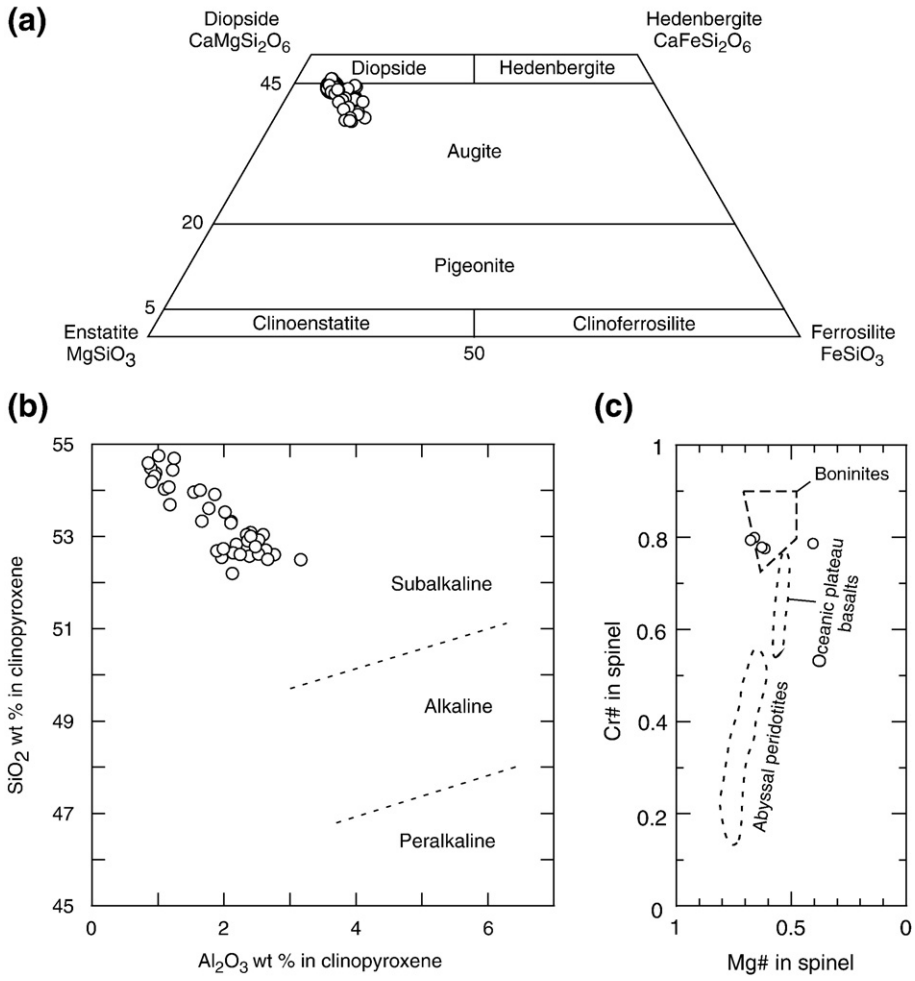

Fig. 6. (a) Composition of the Southern Deep clinopyroxene (circle) plotted in pyroxene quadrilateral by Morimoto et al. (1988). Note that data from a single sample are plotted. (b) Plot of SiO_2 wt.% vs. Al_2O_3 wt.% for the Southern Deep clinopyroxene (circle). Note that data from a single sample are plotted. Boundaries after Le Bas (1962). (c) Mg# (=Mg/(Mg+Fe)) vs. Cr# (=Cr/(Cr+Al)) for the Southern Deep spinel (circle) (a single sample). Fields for boninites, oceanic plateau basalts, and abyssal peridotites from Dick and Bullen (1984).

magma (which is SiO_2-oversaturated) have higher contents of Si and lower contents of Al in the tetrahedral site of the pyroxene structure, whereas those from alkaline magma (which is SiO_2-undersaturated) have lower Si and higher Al contents. Following these works, Nisbet and Pearce (1977) and Leterrier et al. (1982) developed a discriminating method for defining magma type based on statistical analysis on clinopyroxene compositions.

The Southern Deep clinopyroxene clearly plot in the subalkaline field defined by Le Bas (1962) (Fig. 6b). This in turn was confirmed by the Nisbet–Pearce method, resulting in "volcanic arc basalt" or "ocean-floor basalt" (i.e., mid-ocean ridge basalt; MORB) (Nisbet and Pearce, 1977) (figure not shown). Since clinopyroxenes in "within plate alkali basalt" have high Na and Ti, and low Si contents, on the basis of Nisbet–Pearce method, we can confidently rule out the possibility that the Southern Deep clinopyroxene came from "within plate alkali basalt" (Nisbet and Pearce, 1977) (figure not shown). The spinel chemistry further supports our argument. Spinel is a ubiquitous accessory mineral in basalt and peridotite, and is extremely sensitive to bulk composition, mineralogy and petrogenesis of the host rocks (Dick and Bullen, 1984; Arai, 1992). It has been shown in the literature that spinels in island-arc magmas including boninite have very high-Cr# (~>0.8) (Dick and Bullen, 1984; Arai, 1992). This may reflect the high Si and low Al contents of the parental melts (Dick and Bullen, 1984). The southern deep spinel plots in the field for boninites defined by Dick and Bullen (1984) (Fig. 6c). The spinel composition together with the result of the Nisbet–Pearce method suggests that the Southern Deep lava is more like boninite or island-arc tholeiite, not a "within plate alkali basalt" like an OIB (Ocean Island Basalt), nor MORB.

5. Discussions

5.1. Southern extension of the main Parece Vela Basin and its genetic relationship with Yap arc

The southern tip of the PVB and the Yap Trench show a unique tectonic setting and geometry. According to previous

studies, the collision of the Caroline Ridge played an important role in the development of the Yap arc and backarc region. Based on geophysical data along the Yap Trench, Fujiwara et al. (2000) suggested that the shallow part of the landward side of the trench may consist of the obducted PVB which is bent upward. Submersible dives at landward wall of the trench reveals the existence of thrusts in the lower crust (Fujioka et al., 1996), supporting the idea that the PVB oceanic crust has overridden the pre-existed Yap arc. Metamorphosed rocks and gabbros of PVB origin predominate in the Yap Islands (Shiraki, 1971) and the upper part of the forearc. Based on these facts Ohara et al. (2002) revised the history of the Yap arc system. According to their hypothesis, the evolution can be described by four stages: 1) the eruption of proto-Yap–Mariana forearc at 50–40 Ma, 2) the southward propagation of the PVB spreading and incipient arc magmatism from the propagating tip of PVR at ~25 Ma, 3) the collision of the Caroline Ridge and the obduction of PVB crust over the proto-Yap arc, 4) the extensive erosion of Yap forearc during subsequent subduction. However, they do not show the strong evidence supporting such a southward propagation of the spreading axis.

Our results provide additional constraints on the evolution of the southern PVB. First, our study clearly shows that the main PVB extends south up to 9°20′N along the Yap arc. A spreading fabric indicating NE–SW extension is observed west of the Yap Islands. Also the fracture zones which continued from the fossil rift (PVR) at 12°N are recognized. Such observations suggest that the NE–SW spreading stage that occurred in the main PVB also occurred in its southernmost part and that the western half of the seafloor formed during this stage has been mostly preserved. The relatively higher Bouguer gravity anomalies in this area tend to show that no thick arc crust exists despite its shallow depth. However, we do not find a strong geophysical evidence for the obduction of the PVB.

Second, widespread N–S trending abyssal hills are observed in the northern part of the survey area. They are morphologically similar to the western half of the main PVB (Okino et al., 1998), as shown by similar wavelength of abyssal hills and by the lack of prominent fracture zones. This area, therefore, very likely formed during the E–W spreading stage. The southeastern boundary of the area of N–S lineaments (~9°20′N) adjoins NW–SE spreading fabrics. Such an observation suggests that the eastern counterpart, which was formed during the E–W spreading stage, has moved northeastward along the NE–SW fracture zones, and that it is now located west of the present-day West Mariana Ridge. This motion could have also displaced the original Yap Trench. In this instance, the subduction did not erode the eastern half of southern PVB.

Third, there is no evidence for large-scale southward rift propagation during the early (i.e., E–W spreading) stage of basin formation. Although the structure of the boundary between the arc and the basin is not so clear in study area, the width of basin floor with N–S abyssal hills is almost constant all over the southern PVB. It seems that the propagation occurred at the tip of N–S spreading segment in the late stage of E–W spreading and produced the short NW–SE trending pseudofault that separates N–S and NW–SE trending fabrics.

5.2. Tectonics of the southernmost PVB

Unlike the spreading fabric in the main PVB and the northern part of the study area behind the northern Yap arc, the southernmost PVB displays a complex morphology. Prominent curvilinear deeps and a series of rifts exist, and a large relatively shallow seafloor with multiple topographic highs is found between the deeps. No clear spreading fabric can be recognized in this shallow area, suggesting that pre-existing volcanic constructions were deformed during the rifting.

The northern curvilinear deep dissects the KPR crust. It also cuts across the N–S abyssal hills which extended from the main PVB, suggesting that the deep may have formed a few million years after the initiation of E–W spreading in the main PVB. The 080° fabric may be the result of the interaction between N–S trending spreading axis propagated from the north and the southernmost rift system. The curvilinear rifts, the shallow area between rifts, and the adjacent fabric indicative of rotation all resemble the morphological features reported in other regions that have undergone substantial amount of rotation such as Pito Deep in the northeastern margin of Easter Microplate (Martinez et al., 1991; Naar and Hey, 1991; Hey et al., 2002) and the Endeavor Deep in northeastern margin of the Juan Fernandez Microplate (Larson et al., 1992; Kleinrock and Bird, 1994). The complex structures are attributed to the rotation, where two spreading axes separated by large distance overlap and the rift propagated into ~3 Myr.-old pre-existing crust. These microplates have developed along the fast-spreading ridges; on the other hand, the E–W spreading in the main PVB occurred at intermediate rate (average half rate=40 mm/yr. by Okino et al. (1998); half rate ranges 24–58 mm/yr. by Sdrolias et al. (2004)). Our study also differs with those regions in that it lies in a backarc setting. Still a similar stress regime may have caused the curvilinear rifts in the southernmost PVB.

It appears that when the southernmost Yap backarc was beginning to rift, the opening of the main PVB was already in progression (Fig. 7a). Initially the southernmost Yap backarc may have consisted of Oligocene arc crust and pre-Oligocene remnant crust. The spreading axis of the main PVB gradually propagated to the south and split the pre-existing crust (thick arrow in Fig. 7b). On the other hand, the southernmost PVB may have not controlled by simple E–W extension because of the complicated geometry of the subduction zone and possibly of the influence of the subduction along the Palau arc–trench system, which was active at that time (Cosca et al., 1998). It is possible that another southernmost spreading segment may have developed parallel to the curved Yap Trench (double line in Fig. 7b). The trench changes its direction almost 90° at its southern end such that the related rift system likely formed in the E–W direction. A series of rifts, in the meantime, also developed along the present-day southernmost KPR. This rift system (western rift in Fig. 7b) and the rift that extends from the main PVB began to overlap at first with a large offset, forming curvilinear deeps and rifts. The pre-existing crust between the deeps/rifts also became deformed and was partly uplifted (Fig. 7b). The region showing 080° spreading fabric is thought to have formed

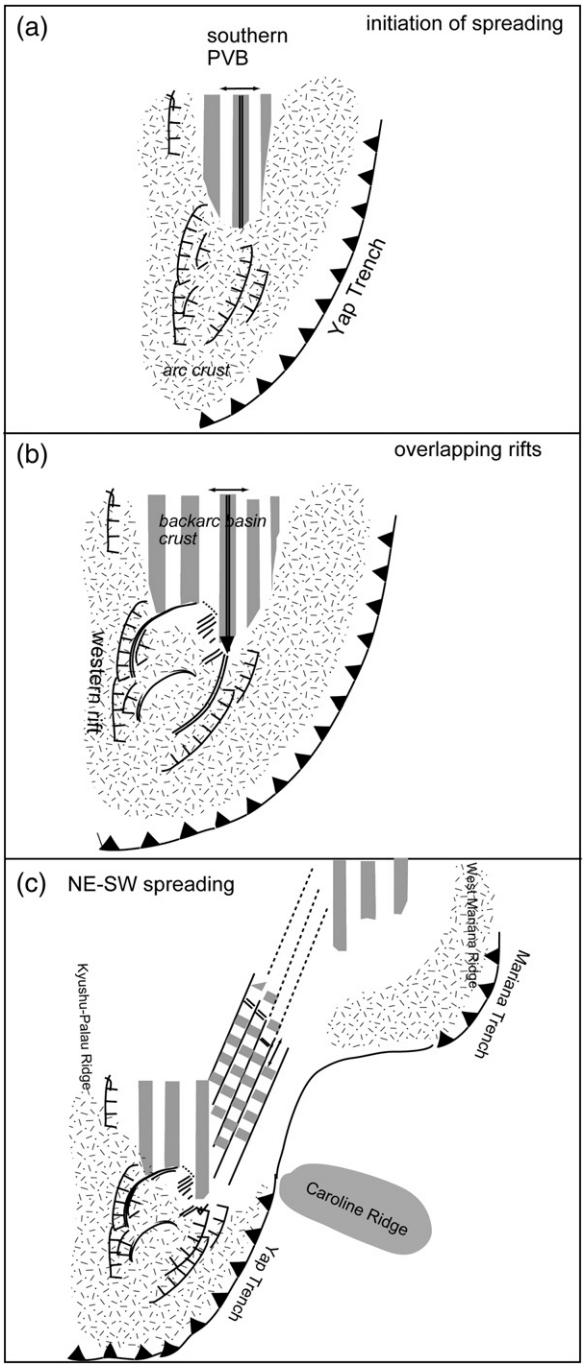

Fig. 7. One hypothesis for the evolution of the southern tip of the PVB. (a) The landward side of the Yap Trench consists of island arc crust and remnant lithosphere inherited from old Philippine Sea. Backarc extension in E–W direction split the arc crust and new oceanic crust was formed. (b) Overlapping rifts developed at the southern tip of the PVB. (c) The southernmost overlapping rift system was abandoned and the NE–SW spreading occurred in the main PVB.

from an unknown E–W trending southernmost segment of the eastern rift system. Small blocks having fabric of variable orientation are also recognized in this region. A similar rotated fabric is often observed at spreading tips where overlapping spreading evolves with a trail of failed rifts or in regions where rotation is the dominant mode of tectonic deformation (Naar and Hey, 1991; Kleinrock and Bird, 1994; Korenaga and Hey, 1996). The western rift including the curved deeps was abandoned when the main PVB was opening in NE–SW direction (Fig. 7c). The eastern flank of the southern PVB have displaced northeastward. Such a motion could have also displaced a part of the original Yap Trench and the southernmost PVB spreading axis would have been replaced by the subduction zone from the south. This hypothesis would explain the short length of the subducted slab beneath the Yap arc and the lack of active Yap arc volcanism without a large amount of subduction erosion that was suggested by previous models (e.g., Ohara et al., 2002).

The evolution of the PVB may have been similar to that of the Mariana Trough in many ways. The central Mariana Trough started to open at 6 Ma at 18°N (e.g., Hussong and Uyeda, 1981; Iwamoto et al., 2002) and propagated north forming the V-shaped structure in the basin (Yamazaki et al., 2003). In the PVB, the spreading started at the middle of the basin and propagated northward (Okino et al., 1998). Both in the PVB and the Mariana Trough, the southernmost regions show a marked difference between their northern and central parts. A systematic southward propagation is not found in both basins. The southern tip of the Mariana Trough has an unusual structure, including a shallow platform, ambiguous rift axis, spreading fabrics of various directions and numerous volcanoes between arc and backarc. Such a diversity is supposed to be influenced probably by the large curvature of the trench (Martinez et al., 2000). The southernmost PVB was also affected by the curved trench system but in a different way. The observed morphological features suggest that the pre-existing crust may have been rifted and the spreading fabrics in various orientations have formed under rotation tectonics between two synchronously active rift systems with a relatively large offset.

The genesis of the complex shallow area between two curvilinear deeps is not fully understood at this moment. The shallow depth and thick crust inferred from gravity anomalies suggests a robust volcanism took place during the formation of this structure. The possible boninitic signature of the rock samples collected at the Southern Deep may support the idea that the robust volcanism may have been influenced by a thermal anomaly. As shallow area was partly deformed and the Northern Deep cuts the N–S abyssal hills, the area presumably consists of pre-Oligocene crust. Although there is no available age data from our survey area, the argument for pre-Oligocene thermal anomaly may be supported by several evidences in other parts of the Philippine Sea Plate. For instance, the rocks collected in the western Philippine Sea show OIB signature (Hickey-Vargas, 1998; Macpherson and Hall, 2001). Middle Eocene boninites were also reported along the IBM forearc (Bloomer et al., 1995). The reconstructed Middle Eocene location of these sites lies close to the present-day Manus Basin where the petrological and geochemical evidence indicate the presence of a mantle plume. The present-day Yap arc area was located near the trace of the Manus plume in Middle Eocene before initiation of PVB rifting and a part of this area may have been affected by a thermal anomaly. Alternatively, the robust volcanism

forming the topographic highs could have occurred at least partly concurrently with the rifting of the southernmost PVB. As the area is close to the volcanic arc to the south, it is possible that some arc-derived magma mixed with magma erupting along the southern tip of the spreading axis. Deschamps and Lallemand (2003) proposed that the intersections between an active spreading center and arc/subduction zone could cause the formation of boninites in backarc basins, in addition to the settings that involve the presence of a mantle plume. The boninitic signature of our sample may be explained by their model.

The proximity of backarc spreading center to active arc may also cause widespread off-axis volcanism between the backarc and arc, which is observed in the southern Mariana Trough (Martinez et al., 2000) and the westernmost Okinawa Trough (Sibuet et al., 1998). Small conical seamounts between the southern deep and the present-day arc may have occurred concurrently with the PVB formation under the influence of arc-backarc interaction.

6. Conclusions

The geophysical and geochemical data collected during our recent survey reveal the structure of the southernmost Parece Vela Basin (PVB) and provide us new information about the evolution of the area.

1. The main PVB extends southward up to 9°20′N along the Yap arc. Both N–S fabric formed during the stage of E–W spreading and NW–SE fabric during the stage of NE–SW spreading that occurred in the main PVB are recognized west of the Yap arc. The fracture zones, which offset the NW–SE abyssal hills, connect to the fossil rift in the main PVB. The eastern counterpart may be located north of the E–W trending southern Mariana Trench.
2. The northern Yap arc and accompanied NW–SE spreading fabric is characterized by a relatively higher gravity anomaly than in the south. This observation may support the hypothesis that the northern Yap arc does not have typical arc crust and that the crust was partly eroded by the subduction. The positive isostatic anomalies in this region might relate to some dynamical effect of the obduction.
3. Prominent curvilinear deeps, a series of rifts and a complex shallow area with multiple topographic highs are discovered in the southernmost part of the PVB. The series of rifts and deeps dissected the southernmost KPR crust and also cut across the local N–S fabric that extended from the main PVB. This observation suggests the rifting along the southernmost KPR occurred a few million years after the initiation of main PVB formation.
4. The southernmost PVB might have formed under the influence of overlapping rift system with a relatively large offset and of the curved geometry of the southern Yap Trench. The western rift system dissecting the southernmost KPR and the eastern rift system propagating from the main PVB overlapped at the southern tip of the Yap backarc, deforming the existing old arc crust.

Acknowledgements

We are grateful to the captain, officers and crew of R/V Hakuho-maru for their experienced work during data acquisition. Yumiko Harigane, Mizuki Watanabe, Hiroyuki Inoue, Yoon-Mi Kim, Taichi Sato and Yaoming Yan are thanked for their collaboration and discussion onboard. We are also indebted to Hideo Ishigaki and Shin'ichiro Yokogawa for their technical support. We deeply thank Teruaki Ishii and Mayumi Otsuki for helping us in performing geochemical analyses. This manuscript benefited greatly from careful reviews by F. Martinez and A. Deschamps. The GMT software (Wessel and Smith, 1995) and MB system (Caress and Chayes, 1996) were extensively used in this study. The study was supported by the Japan Society for the Promotion of Science, Grant-in-Aid for Scientific Researches to K. Okino [(B)16340127]. Cruise participation for S.-M. Lee and Y.-M. Kim was funded by BK21 Program.

References

Arai, S., 1992. Chemistry of chromian spinel in volcanic-rocks as a potential guide to magma chemistry. Mineralogical Magazine 56 (383), 173–184.

Bence, A.E., Albee, A.L., 1968. Empirical correction factors for the electron microanalysis of silicates and oxides. Journal of Geology (76), 382–403.

Bloomer, S.H., Taylor, B., MacLeod, C.J., Stern, R.J., Fryer, P., Hawkins, J.W., Johnson, L., 1995. Early arc volcanism and the ophiolite problem: a perspective from drilling in the western Pacific. In: Taylor, B., Natland, J. (Eds.), Active Margins and Marginal Basins of the Western Pacific. American Geophysical Union Geophysical Monograph, pp. 1–30.

Cande, S.C., Kent, D.V., 1995. Revised calibration of the geomagnetic polarity timescale for the Late Cretaceous and Cenozoic. Journal of Geophysical Research-Solid Earth 100 (B4), 6093–6095.

Caress, D.W., Chayes, D.N., 1996. Improved processing of Hydrosweep DS multibeam data on the R/V Maurice Ewing. Marine Geophysical Researches 18 (6), 631–650.

Christie, D.M., Sinton, J.M., 1981. Evolution of abyssal lavas along propagating segments of the Galapagos Spreading Center. Earth and Planetary Science Letters 56 (DEC), 321–335.

Cosca, M.A., Arculus, R.J., Pearce, J.A., Mitchell, J.G., 1998. Ar-40/Ar-39 and K-Ar geochronological age constraints for the inception and early evolution of the Izu–Bonin–Mariana arc system. Island Arc 7 (3), 579–595.

Deschamps, A., Lallemand, S., 2002. The West Philippine Basin: an Eocene to early Oligocene back arc basin opened between two opposed subduction zones. Journal of Geophysical Research-Solid Earth 107 (B12). doi:10.1029/2001JB001706.

Deschamps, A., Lallemand, S., 2003. Geodynamic setting of Izu–Bonin–Mariana noninites. In: Larter, R.D., Leat, P.T. (Eds.), Intra-oceanic Subduction Systems: Tectonic and Magmatic Processes. Geological Society, London, Special Publications. Geological Society of London, London, pp. 163–185.

Dick, H.J.B., Bullen, T., 1984. Chromian spinel as a petrogenetic indicator in abyssal and alpine-type peridotites and spatially associated lavas. Contributions to Mineralogy and Petrology 86 (1), 54–76.

Fujioka, K., Kobayashi, K., Fujiwara, T., Kitazato, H., Iwabuchi, Y., Tamura, C., Omori, K., Kato, K., Ariyoshi, M., Kodera, T., 1996. Tectonics of southern tip of the Philippie Sea: results of Southerncross '95 cruise. JAMSTEC Journal of Deep Sea Researches 12, 275–290.

Fujiwara, T., Tamura, C., Nishizawa, A., Fujioka, K., Kobayashi, K., Iwabuchi, Y., 2000. Morphology and tectonics of the Yap Trench. Marine Geophysical Researches 21 (1–2), 69–86.

Hall, R., Ali, J.R., Anderson, C.D., Baker, S.J., 1995. Origin and motion history of the Philippine Sea Plate. Tectonophysics 251 (1–4), 229–250.

Haraguchi, S., Ishii, T., Kimura, J.I., Ohara, Y., 2003. Formation of tonalite from basaltic magma at the Komahashi-Daini Seamount, northern Kyushu–Palau Ridge in the Philippine Sea, and growth of Izu–Ogasawara (Bonin)–Mariana arc crust. Contributions to Mineralogy and Petrology 145 (2), 151–168.

Hey, R.N., Martinez, F., Diniega, S., Naar, D.F., Francheteau, J., Armijo, R., Constantin, M., Cogne, J.P., Girardeau, J., Hekinian, R., Searle, R., 2002. Preliminary attempt to characterize the rotation of seafloor in the Pito Deep area of the Easter Microplate using a submersible magnetometer. Marine Geophysical Researches 23 (1), 1–12.

Hickey-Vargas, R., 1998. Origin of the Indian Ocean-type isotopic signature in basalts from Philippine Sea plate spreading centers: an assessment of local versus large-scale processes. Journal of Geophysical Research-Solid Earth 103 (B9), 20963–20979.

Hilde, T.W.C., Lee, C.S., 1984. Origin and evolution of the West Philippine Basin — a new interpretation. Tectonophysics 102 (1–4), 85–104.

Hochstaedter, A.G., Gill, J.B., Taylor, B., Ishizuka, O., Yuasa, M., Morita, S., 2000. Across-arc geochemical trends in the Izu–Bonin arc: constraints on source composition and mantle melting. Journal of Geophysical Research-Solid Earth 105 (B1), 495–512.

Hussong, D.M., Uyeda, S., 1981. Tectonic processes and the history of the Mariana Arc, a synthesis of the results of Deep Sea Drilling Project leg 60, Initial Report of Deep Sea Drilling Project, pp. 909–929.

Ishizuka, O., Taylor, R.N., Milton, J.A., Nesbitt, R.W., 2003. Fluid–mantle interaction in an intra-oceanic arc: constraints from high-precision Pb isotopes. Earth and Planetary Science Letters 211 (3–4), 221–236.

Iwamoto, H., Yamanoto, M., Seama, N., Kitada, K., Matsuno, T., Nogi, Y., Goto, T., Fujiwara, T., Suyehiro, K., Yamazaki, T., 2002. Tectonic evolution of the central Mariana Trough. EOS Trans. AGU 83 (47) Fall Meet. Suppl., Abstract T72A-1235.

Karig, D.E., 1971. Origin and development of marginal basins in western Pacific. Journal of Geophysical Research 76 (11), 2542–2561.

Kleinrock, M.C., Bird, R.T., 1994. Southeastern boundary of the Juan-Fernandez microplate — braking microplate rotation and deforming the Antarctic plate. Journal of Geophysical Research-Solid Earth 99 (B5), 9237–9261.

Korenaga, J., Hey, R.N., 1996. Recent dueling propagation history at the fastest spreading center, the East Pacific Rise, 26 degrees-32 degrees S. Journal of Geophysical Research-Solid Earth 101 (B8), 18023–18041.

Kotake, Y., 2000. Study on the tectonics of western Pacific region derived from GPS data analysis, 75. Bulletin of Earthquake Researth Institute, University of Tokyo, pp. 229–334.

Kushiro, I., 1960. Si–Al relation in clinopyroxene from igneous rocks. American Journal of Science 258, 548–554.

Larson, R.L., Searle, R.C., Kleinrock, M.C., Schouten, H., Bird, R.T., Naar, D.F., Rusby, R.I., Hooft, E.E., Lasthiotakis, H., 1992. Roller-bearing tectonic evolution of the Juan-Fernandez microplate. Nature 356 (6370), 571–576.

Le Bas, M.J., 1962. The role of aluminum in igneous clinopyroxenes with relation to their parentage. American Journal of Science 260, 267–288.

Lee, S.M., 2004. Deformation from the convergence of oceanic lithosphere into Yap Trench and its implications for early-stage subduction. Journal of Geodynamics 37 (1), 83–102.

Leterrier, J., Maury, R.C., Thonon, P., Girard, D., Marchal, M., 1982. Clinopyroxene composition as a method of identification of the magmatic affinities of paleovolcanic series. Earth and Planetary Science Letters 59 (1), 139–154.

Machida, S., Ishii, T., 2003. Backarc volcanism along the en echelon seamounts: the Enpo seamount chain in the northern Izu–Ogasawara arc. Geochemistry Geophysics Geosystems 4. doi:10.1029/2003GC000554.

Macmillan, S., Maus, S., Bondar, T., Chambodut, A., Golovkov, V., Holme, R., Langlais, B., Lesur, V., Lowes, F., Luhr, H., Mai, W., Mandea, M., Olsen, N., Rother, M., Sabaka, T., Thomson, A., Wardinski, I., 2003. The 9th-generation international geomagnetic reference field. Geophysical Journal International 155 (3), 1051–1056.

Macpherson, C.G., Hall, R., 2001. Tectonic setting of Eocene boninite magmatism in the Izu–Bonin–Mariana forearc. Earth and Planetary Science Letters 186 (2), 215–230.

Martinez, F., Naar, D.F., Reed, T.B., Hey, R.N., 1991. 3-dimensional seamarc Ii, gravity, and magnetics study of large-offset rift propagation at the Pito Rift, Easter Microplate. Marine Geophysical Researches 13 (4), 255–285.

Martinez, F., Fryer, P., Baker, N.A., Yamazaki, T., 1995. Evolution of backarc rifting—Mariana Trough, 20-Degrees-N-24-Degrees-N. Journal of Geophysical Research-Solid Earth 100 (B3), 3807–3827.

Martinez, F., Taylor, B., Goodliffe, A.M., 1999. Contrasting styles of seafloor spreading in the Woodlark Basin: indications of rift-induced secondary mantle convection. Journal of Geophysical Research-Solid Earth 104 (B6), 12909–12926.

Martinez, F., Fryer, P., Becker, N., 2000. Geophysical characteristics of the southern Mariana Trough, 11 degrees 50 ′ N-13 degrees 40 ′ N. Journal of Geophysical Research-Solid Earth 105 (B7), 16591–16607.

McCabe, R., Uyeda, S., 1983. Hypothetical model for the bending of the Mariana Arc. In: Hayes, D.E. (Ed.), The tectonic and geologic evolution of southeast Asian Seas and Islands, 2. AGU Geophysical Monograph Series, pp. 281–293.

Morimoto, N., Fabries, J., Ferguson, A.K., Ginzburg, I.V., Ross, M., Seifert, F.A., Zussman, J., Aoki, K., Gottardi, G., 1988. Nomenclature of pyroxenes. American Mineralogist 73, 1123–1133.

Mrozowski, C.L., Hayes, D.E., 1979. Evolution of the Parece Vela Basin, Eastern Philippine Sea. Earth and Planetary Science Letters 46 (1), 49–67.

Naar, D.F., Hey, R.N., 1991. Tectonic evolution of the Easter Microplate. Journal of Geophysical Research-Solid Earth and Planets 96 (B5), 7961–7993.

Nisbet, E.G., Pearce, J.A., 1977. Clinopyroxene composition in mafic lavas from different tectonic settings. Contributions to Mineralogy and Petrology 63 (2), 149–160.

Ohara, Y., Ishii, T., Fujioka, K., Kato, Y., Haraguchi, S., Kasuga, S., Sasaki, T., Kanamatsu, T., Sakamoto, I., 1997. Report of multi-channel seismic reflection and submersible Shinkai 6500 studies at Kyushu–Palau Ridge. Report of Hydrographic Researches 33, 85–93.

Ohara, Y., Yoshida, T., Kato, Y., 2001. Giant Megamullion in the Parece Vela Backarc Basin. Marine Geophysical Researches 22, 47–61.

Ohara, Y., Fujioka, K., Ishizuka, O., Ishii, T., 2002. Peridotites and volcanics from the Yap arc system: implications for tectonics of the southern Philippine Sea Plate. Chemical Geology 189 (1–2), 35–53.

Ohara, Y., Okino, K., Snow, J.E., KR03-01 Shipboard Scientific Party, 2003. Preliminary report of Kairei KR03-01 cruise: amagmatic tectonics and lithospheric composition of the Parece Vela Basin. InterRidge News 12 (1), 27–29.

Ohara, Y., Okino, K., Snow, J.E., Hellebrand, E., Harigane, Y., Michibayashi, K., Ishizuka, O., 2005. Crustal accretion in the Parece Vela Backarc basin: the world's fastest ultraslow-spreading ridge. 2005 American Geophysical Union Fall Meeting: T33G-07.

Okino, K., Shimakawa, Y., Nagaoka, S., 1994. Evolution of the Shikoku Basin. Journal of Geomagnetism and Geoelectricity 46 (6), 463–479.

Okino, K., Kasuga, S., Ohara, Y., 1998. A new scenario of the Parece Vela Basin genesis. Marine Geophysical Researches 20 (1), 21–40.

Okino, K., Ohara, Y., Kasuga, S., Kato, Y., 1999. The Philippine Sea: new survey results reveal the structure and the history of the marginal basins. Geophysical Research Letters 26 (15), 2287–2290.

Parker, R.L., 1972. Rapid calculation of potential anomalies. Geophysical Journal of the Royal Astronomical Society 31 (4), 447–455.

Sandwell, D.T., Smith, W.H.F., 1997. Marine gravity anomaly from Geosat and ERS 1 satellite altimetry. Journal of Geophysical Research-Solid Earth 102 (B5), 10039–10054.

Sdrolias, M., Roest, W.R., Muller, R.D., 2004. An expression of Philippine Sea plate rotation: the Parece Vela and Shikoku Basins. Tectonophysics 394 (1–2), 69–86.

Seno, T., Stein, S., Gripp, A.E., 1993. A model for the motion of the Philippine Sea Plate consistent with Nuvel-1 and geological data. Journal of Geophysical Research-Solid Earth 98 (B10), 17941–17948.

Shinohara, M., Takahashi, N., Li, K., Suyehiro, K., Taira, A., 1999. Crustal structure of the norhtern Izu–Ogasawara arc and the northern Kyushu–Palau Ridge. Chikyu Monthly X23, 67–78.

Shiraki, K., 1971. Metamorphic basement rocks of Yap Islands, Western Pacific — possible oceanic crust beneath an island arc. Earth and Planetary Science Letters 13 (1), 167–174.

Sibuet, J.C., Deffontaines, B., Hsu, S.K., Thareau, N., Le Formal, J.P., Liu, C.S., 1998. Okinawa trough backarc basin: early tectonic and magmatic evolution. Journal of Geophysical Research-Solid Earth 103 (B12), 30245–30267.

Sinton, J.M., Wilson, D.S., Christie, D.M., Hey, R.N., Delaney, J.R., 1983. Petrologic consequences of rift propagation on oceanic spreading ridges. Earth and Planetary Science Letters 62 (2), 193–207.

Tamaki, K., 1992. Formation process of the Japan Sea — a new model of backarc basin opening. Kagaku 11, 720–729.

Taylor, B., Klaus, A., Brown, G.R., Moore, G.F., Okamura, Y., Murakami, F., 1991. Structural development of Sumisu Rift, Izu–Bonin Arc. Journal of Geophysical Research-Solid Earth 96 (B10), 16113–16129.

Tokuyama, H., 1995. Origin and development of the Philippine Sea. In: Tokuyama, H., et al. (Ed.), Geology and Geophysica of the Philippine Sea. Japan-Russia-China Monograph. Terra Scientific Publishing Company, Tokyo, pp. 155–163 (JRCM) (TERRAPUB).

Wessel, P., Smith, W.H.F., 1995. New version of Generic Mapping Tools released. EOS Trans. AGU 76, 329.

Yamazaki, T., Seama, N., Okino, K., Kitada, K., Naka, J., 2003. Spreading process of the northern Mariana Trough: rifting–spreading transition at 22 degrees N. Geochemistry Geophysics Geosystems 4 art. no.-1075.